Acta Polytechnica **64**(6):487–500, 2024
https://doi.org/10.14311/AP.2024.64.0487

Published by the Czech Technical University in Prague

ASSESSMENT OF THE EFFECTS OF UV-A EXPOSURE ON THE MECHANICAL STRENGTH OF OFFSHORE MOORING MULTIFILAMENTS

Daniel Magalhães da Cruz[a,*], Felipe Tempel Stumpf[a], Jakson Manfredini Vassoler[a], Carlos Eduardo Marcos Guilherme[b]

[a] *Federal University of Rio Grande do Sul (UFRGS), Graduate Program in Mechanical Engineering (PROMEC), Applied Mechanics Group (GMAp), 90050-170 Porto Alegre/RS, Brazil*

[b] *Federal University of Rio Grande (FURG), Engineering School (EE), Stress Analysis Laboratory Policab, 96203-000 Rio Grande/RS, Brazil*

[*] corresponding author: daniel.cruz@ufrgs.br

Abstract. The offshore industry faces significant challenges in the dynamic energy and maritime domain, necessitating robust engineering solutions for mooring systems. This study investigates the impact of ultraviolet radiation A (UV-A) on the mechanical strength of high-strength multifilaments, crucial for offshore mooring. Five fibre types: Aramid, High-modulus polyethylene (HMPE), Liquid crystal polymers (LCP), Polyamide and Polyester, are exposed to UV-A for up to 28 days. Initial mechanical characterisation provides baseline data, while subsequent tests reveal varying degrees of degradation. Polyamide and polyester exhibit superior stability, while Aramid and HMPE show restrained degradation. LCP experiences substantial degradation. Mathematical modelling reveals distinct degradation patterns, emphasising the need for comprehensive understanding in ensuring the safety and efficiency of offshore operations. There are indications that degradation by ultraviolet exposure for Aramid, HMPE, polyamide, and polyester fibres, restricts the constitutive behaviour in terms of strength and extension, but without changing the shape of the curve. These findings provide valuable insights for the offshore industry and guidance future research and development efforts.

Keywords: Tensile testing, mechanical characterisation, ultraviolet incidence, degradation, synthetic fibres, yarn break load, curve fitting modelling.

1. Introduction

The offshore industry can be seen as one of the most challenging and dynamic sectors within the energy and maritime domain. With the continuous development of new technologies and techniques, operations in deep and ultra-deep waters are becoming increasingly feasible. However, the extreme environment requires robust engineering solutions, including reliable mooring systems that are pivotal for the safety and stability of offshore structures (especially for Floating Offshore Wind Turbines). A fundamental component of a mooring system is high strength multifilaments, which play a critical role in the station-keeping of floating structures that have to withstand adverse environmental conditions.

In this context, offshore mooring systems have evolved considerably in recent decades, with one of the most notable changes being the transition from traditional steel wire cables to high-tenacity synthetic polymeric fibres. This revolutionary shift, initially proposed by Del Vecchio in the 1990s [1], introduced taut-leg mooring systems with synthetic fibres, marking a significant innovation over conventional steel catenaries. Synthetic ropes offer several desirable properties, including low weight, high strength, flexibility, low friction coefficient, and resistance to aggressive marine conditions [2–4]. Today, these polymeric multifilaments, mainly polyester, are widely adopted in mooring systems, solidifying their role as an essential material for the offshore industry [5–12].

This technological novelty and the inherent characteristics of synthetic fibres have led to various advancements in commercial, professional, and academic domains. These materials are extensively examined through analytical [13–17], numerical [18–26], and experimental [4, 10, 12, 27–37] approaches due to their critical significance for the integrity and efficiency of offshore operations. Many studies have addressed the use of fibres for offshore mooring, covering a wide range of loading conditions, environmental settings, fibre types, stiffness analysis, and physical properties.

A fundamental challenge in the offshore industry is the constant exposure to adverse environmental conditions, with ultraviolet (UV) radiation being a noticeable concern. These rays, particularly UV-A radiation, can significantly affect polymeric materials, including multifilaments used in mooring systems. A prolonged exposure to UV-A rays can lead to the degradation and weakening of polymers, thereby compromising their mechanical strength [38–40]. This potential degradation threatens the integrity of mooring systems and, consequently, the safety of offshore operations.

Property	Aramid	HMPE	LCP	Polyamide	Polyester
Density [g cm^{-3}]	1.44	0.97	1.40	1.14	1.38
Melting point [°C]	500	150	400	218	258
Glass transition [°C]	145	50	120	60	75
Modulus [N tex^{-1}]	60	100	54	7	11
Tenacity [N tex^{-1}]	2	3.5	2.29	0.84	0.82
Break strain [%]	∼4	∼3.5	∼4	18∼21	11∼13
Moisture [%]	1∼7	0	<0.1	5	<1

Table 1. General properties of high-performance synthetic fibres.

Numerous studies have investigated the mechanical strength of polymeric fibres under ideal laboratory conditions [4, 9, 12, 29, 32–36, 41]. However, only a few studies have explored the impact of UV exposure on the strength of synthetic fibres. Most of the studies related to UV exposure have focused on composite matrices [42–44], glass fibres [45–47], and plant-based fibres [48, 49]. To the author's knowledge, very few studies have directly addressed UV exposure in the offshore sector. Therefore, there is an urgent need for a comprehensive analysis to evaluate the effects of UV-A radiation on the mechanical strength of multifilaments specifically designed for offshore mooring, with the aim of providing valuable insights for the industry. At the same time, it allows the characterisation of virgin fibres for each material, which can be compared with fibres from different sectors, such as surgical sutures [50–52], concrete and asphalt additives [53, 54], mountaineering or rescue ropes [55, 56], and fishing lines [57, 58].

This article aims to investigate how exposure to UV-A affects the mechanical tensile strength and rupture characteristics of multifilaments used for making mooring ropes. The study is an exploratory one and uses custom-built UV exposure equipment. The research involves testing five types of fibres: Aramid, High Modulus Polyethylene (HMPE), Liquid Crystal Polymer (LCP), polyamide, and polyester. The UV exposure times range from one to twenty-eight days, with the filaments being removed every seven days for testing.

This experimental study aims to deepen our understanding of the mechanical degradation of mooring materials caused by exposure to UV-A radiation. Additionally, it seeks to investigate the impact of ultraviolet radiation on isolated synthetic fibres. To complement the experimental findings, mathematical models are used to simulate and predict the behaviour of the materials being studied. These models serve as powerful tools to analyse complex phenomena by providing a quantitative framework for interpreting data, identifying trends, and estimating parameters that describe the material behaviour. Their application contributes to a deeper understanding of the degradation processes and offers insights that can guide further research development and help with material selection for specific applications. The results of the study may act as a catalyst for further research in related areas.

2. Materials and methods

2.1. Materials

All fibres investigated in the study are specific for manufacturing offshore mooring ropes and/or other marine applications. There was no authorisation to disclose the fibre codes or their manufacturers.

In any case, it is important to highlight their main characteristics in general, as well as other prominent applications. Table 1, provides some information on the mechanical and physical properties of synthetic fibres in general as reported in the literature [33, 59, 60].

2.1.1. Aramid

Aramid fibres stand out due to their remarkable mechanical properties. They are stronger than steel in terms of tensile strength. Furthermore, they exhibit good impact resistance while possessing a certain lightweight quality. This combination of strength, impact resistance, and lightness makes them ideal for applications such as bulletproof vests [61, 62].

Aramid has been used in mooring systems in the past, but its high cost compared to other fibres, and issues related to axial compression and abrasion resistance hindered its continued use for mooring ropes [60, 63]. It is still used in other maritime applications, particularly in lifting straps on ships and in applications where the fibre is exposed to high environmental temperatures.

2.1.2. High modulus polyethylene (HMPE)

High-modulus polyethylene is renowned for its exceptional tensile strength and lightness [3, 64, 65]. These fibres offer high specific tensile strength when compared to other typical materials, meaning they are strong for their weight. As shown in Table 1, their density is lower than that of water, giving them buoyancy and low moisture absorption. Their limitations are typically associated with higher temperatures and the creep phenomenon.

There are studies in the literature that address the use of HMPE for mooring systems of Mobile Offshore Drilling Units (MODU) [64, 65]. Additionally, there are studies focused on fibres designated as "Low

Creep" [37, 66]. Considering an entire mooring system made of HMPE, with its low elongation, would allow for even greater depths without compromising the platform offset. It is one of the most promising fibres, albeit with a higher specific cost [60]. Other applications of HMPE fibres include the manufacture of ballistic vests [67], mesh for lifting slings in load handling operations [68], among others.

2.1.3. Liquid crystal polymer (LCP)

Liquid crystal polymer fibres are recognized for their high strength and rigidity. They can maintain their dimensional shape over a wide range of temperatures, making them ideal for applications requiring dimensional stability. These fibres can withstand high temperatures, making them valuable in heat-resistant applications. Their low thermal expansion is also important, ensuring that the fibres maintain their structural integrity under temperature variations, making LCP a strategic choice for components subjected to significant temperature changes [69].

LCP fibres are frequently used in applications where extended low creep elongation and/or abrasion resistance is needed for rope and cordage. Examples include mooring tethers, tension ropes, actuator cables, for example, as used in robotics, and other specialty rope/cordage applications [70, 71].

2.1.4. Polyamide

Polyamide (PA), is renowned for its tenacity, elasticity, and wear resistance. It exhibits strong mechanical properties, including high abrasion resistance. As shown in Table 1, it has the highest elongation among the presented fibres. Due to its flexibility, polyamide is frequently used in products requiring elasticity, such as sportswear and stockings [72].

Polyamide fibre can absorb a high number of dynamic loads, precisely because of its high elasticity, which is why it is also used in climbing, operation, and rescue ropes [73]. Its ability to absorb impacts (dynamic load) is discussed in the literature [32, 74]. In offshore mooring applications, polyamide stands out for Floating Offshore Wind Turbine (FOWT) systems, as it effectively addresses the challenges posed by wave mechanics, tidal movements, winds, and waves [59, 75].

2.1.5. Polyester

Polyester (polyethylene terephthalate, PET) is renowned for its versatility and a wide range of desirable properties. Its low cost and ease of processing also contribute to its extensive application across various sectors [60].

It is used in the textile industry for clothing, household fabrics, curtains, among others, because of its durability, wear resistance, and ability to resist wrinkling and fading [76].

In technical applications related to engineering, it is used in straps, various types of safety belts, and belts. In the offshore industry, it is the most commonly used fibre in mooring systems, with a considerable body of literature on its use in this application [5–12, 15, 18–20, 29, 35, 36]. It is also interesting to highlight how the fibre has evolved over the years; decades ago, the linear tenacity of polyester was around $0.60\,\mathrm{N\,tex^{-1}}$, whereas today, this linear tenacity value has reached $0.85\,\mathrm{N\,tex^{-1}}$.

2.2. Ultraviolet exposure

In the literature, several standards address UV exposure under related conditions, but there is no specific standard for ultraviolet exposure in high-performance synthetic fibres for the offshore industry. ASTM G155 [77] focuses on exposing non-metallic materials to UV radiation using xenon arc lamps that simulate solar exposure. ASTM D4329 [78] tests the UV degradation resistance of plastics using fluorescent UV lamps, and ISO 4892 [79] provides broader methods for exposure to laboratory light sources, including UV light, for testing plastics. There are other specific standards aimed at textile fibres, such as ASTM D5035 [80], which may be relevant for assessing the UV resistance of textile fibres.

Due to the lack of a consolidated method for UV exposure of high-performance synthetic fibres for the offshore industry, a cost-effective custom equipment was designed, taking into account the overview from the mentioned standards. Geometrically, it has a rectangular shape and is coated with aluminum foil (for light reflection). It features four ultraviolet lamps arranged on the top (lid) and four on the bottom. The samples are exposed at the geometric centre of the height, with a distance of 32 centimetres between the samples and the upper emission points and the same distance for the lower emission points. Figure 1 shows the equipment used.

Regarding the lamps, UV-A ultraviolet lamps were used, which are particularly useful for comparing different types of polymers. UV-A lamps have no wavelengths shorter 295 nm and do not degrade materials as quickly as UV-B lamps. The specification of the lamp used is the "UVA-340" from Q-Lab [81], which provides the best possible simulation of sunlight in the critical short-wavelength region between 295–365 nm, with an emission peak at 340 nm and irradiance of $0.68–0.89\,\mathrm{W\,m^{-2}\,nm^{-1}}$, Figure 2 [81].

The sample groups for each fibre in relation to UV exposure time contain 10 specimens each and are shown in Table 2. The groups indicated as "0 days" will serve as reference data for mechanical testing and refer to the virgin condition (without UV exposure). In the case of HMPE and polyamide fibres, they have a smaller number of exposure groups due to material quantity limitations. The solution was to maintain a total exposure period of 28 days while sacrificing intermediate times (7 and 21 days).

Figure 1. Low-cost equipment for UV exposure for fibres.

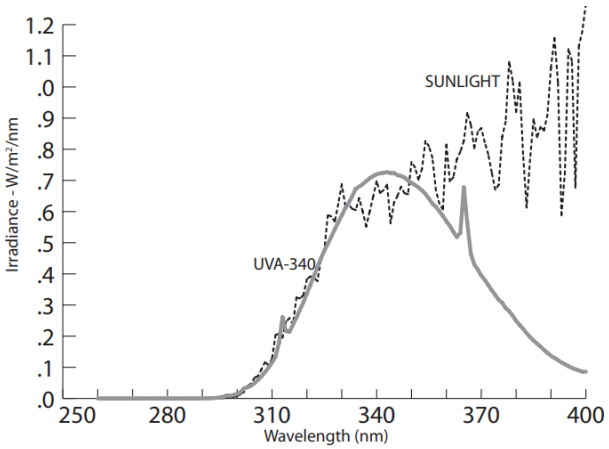

Figure 2. Wavelength of UVA-340 lamp from Q-Lab.

	Aramid	HMPE	LCP	PA	PET
UV [day]	0	0	0	0	0
	7	-	7	-	7
	14	14	14	14	14
	21	-	21	-	21
	28	28	28	28	28

Table 2. Ultraviolet exposure times for each fibre.

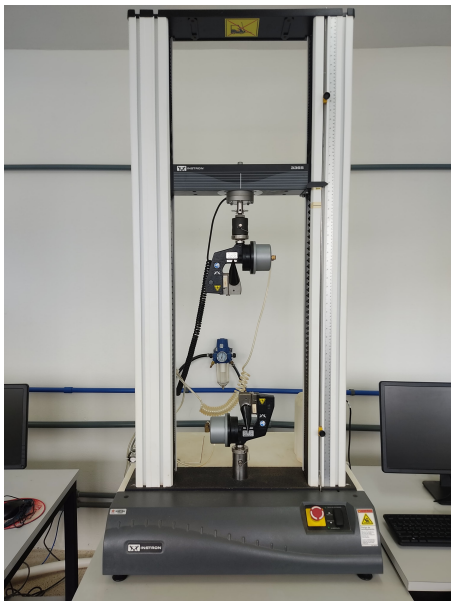

Figure 3. Instron 3365 Equipment for Yarn Break Load tests.

2.3. Mechanical characterisation

The initial mechanical characterisation is performed on all fibres for linear density, tensile strength, and linear tenacity, with data constituting the reference baseline, conducted for virgin conditions without UV exposure. The remaining mechanical characterisation tests refer to the tensile tests performed on specimens after UV degradation.

The linear density testing procedure is standardised by ASTM D1577 [82] and is performed according to ISO 139 [83]. The linear density test is conducted on 10 samples without UV exposure, with a length of 1 000 millimetres and a stabilisation time on a precision scale of 9 minutes. The results are reported in terms of mass per unit length, with the standard unit being tex, representing the weight (in grams) for 1 000 metres of multifilament.

The tensile test is standardised by ISO 2062 [84] and is performed according to ISO 139 [83]. This test, which leads to the fibres' Yarn Break Load (YBL), requires an effective length of 500 millimetres, uniform twist conditions of 60 turns per metre, with a constant extension rate of 250 millimetres per minute. The test is performed using Instron 3365 universal testing machine (Figure 3), capturing the force and extension data during the tensile test. This test will be performed for all conditions specified in Table 2.

Model	Non-Linear Form	Linear Form
Linear	-	$y = B + A \cdot x$
Power	$y = B \cdot x^A$	$\ln y = \ln B + A \cdot \ln x$
Exponential	$y = B \cdot e^{A \cdot x}$	$\ln y = \ln B + A \cdot x$
Reciprocal	$y = (B + A \cdot x)^{-1}$	$y^{-1} = B + A \cdot x$
Michaelis-Menten	$y = A \cdot x \cdot (B + x)^{-1}$	$y^{-1} = A^{-1} + B \cdot (A \cdot x)^{-1}$

TABLE 3. Models used and their linearisation.

Property	Aramid	HMPE	LCP	PA	PET
Linear density [tex]	344.80	185.40	178.50	280.10	339.60
Break strength [N]	631.53	569.98	416.49	198.07	261.15
Stress [MPa]	2 655.78	2 982.10	3 266.56	806.12	1 061.22
Break extension [mm]	20.36	17.01	21.03	87.67	67.90
Break strain [%]	4.07	3.40	4.21	17.53	13.58
Linear tenacity [N tex^{-1}]	1.832	3.074	2.333	0.707	0.769

TABLE 4. Mechanical results of initial fibre characterisation (without UV exposure).

The breaking force value can also be expressed in terms of stress. Due to the inherent difficulty in accurately determining the cross-section of a set of multifilaments, the stress calculation (σ) is based on rupture force (F), linear density (ρ_L), and material density or specific mass (ρ), as illustrated in Equation (1):

$$\sigma\,[\mathrm{MPa}] = \frac{F\,[\mathrm{N}] \times \rho\,\left[\mathrm{g\,cm^{-3}}\right]}{\rho_L\,[\mathrm{g\,m^{-1}}]}. \tag{1}$$

Densities represent the intrinsic physical properties of the material, and the density values indicated in Table 1 are used for this purpose.

2.4. Curve fitting

In the evaluation of the experimental data, especially when characterising a quantity in relation to varying conditions – specifically, stress and/or strain in this case – associated with the increase in time under UV exposure, there is a natural inclination to pursue mathematical modelling of the behaviour. In this study, this type of determination can be a comparative criterion among different types of fibres under UV exposure.

This mathematical parameterisation can be performed simply and effectively using the Least Squares Method (LSM), combined with the mathematical technique of model linearisation. The LSM identifies the parameters of a model that minimise the sum of the squares of the differences between the observed values and those predicted by the model [85, 86]. For this study, we propose working with the following models: linear, power, exponential, reciprocal, and Michaelis-Menten, as listed in Table 3 along with their linearised expressions, using an open-source code available in the literature [87].

For linear fits, the criterion demonstrating the quality of the fit is the coefficient of determination (R^2), which ranges from 0 to 1, the closer it is to 1, the better the fit. The direct mathematical definition for the coefficient of determination is obtained through Equation (2):

$$R^2 = 1 - \frac{\sum (y_i - y_i')^2}{\sum (y_i - \bar{y})^2}, \tag{2}$$

where

y_i are the observed values,

y_i' are the predicted values,

$\bar{y}$ is the mean of the y_i values.

3. Results and discussion

The linear density and initial mechanical results in terms of break strength, stress, break extension, break strain, and linear tenacity were obtained according to [82–84] and are presented in Table 4, for all the fibres under investigation. The values presented in Table 4 correspond to the initial condition (0 days of ultraviolet exposure).

The overall results of different ultraviolet exposure conditions are presented in Table 5, including information on strength and extension for the YBL test. The values presented are the averages corresponding to the samples for each condition. Due to quantitative sample restrictions, the groups of 7 and 21 days of ultraviolet exposure were not performed for HMPE and polyamide.

In the direct observation of the presented results, the LCP fibre values stand out. As the exposure times to ultraviolet radiation increase, the mechanical properties in the rupture test decrease substantially. Figures 4 and 5 show the evolution of the rupture force and extension along UV exposure time, respectively.

When observing the obtained graphs, especially the rupture force *versus* ultraviolet exposure, it can be noted that polyamide and polyester samples exhibit

	Property	0 days	7 days	14 days	21 days	28 days
Aramid	Force [N]	631.53	603.31	559.21	516.69	503.60
	Stress [MPa]	2 655.78	2 537.11	2 351.68	2 172.87	2 117.81
	Extension [mm]	20.36	20.38	19.13	18.13	17.61
	Strain [%]	4.07	4.08	3.83	3.63	3.52
HMPE	Force [N]	569.98	-	529.83	-	499.19
	Stress [MPa]	2 982.10	-	2 772.03	-	2 611.72
	Extension [mm]	17.01	-	15.43	-	14.96
	Strain [%]	3.40	-	3.09	-	2.99
LCP	Force [N]	416.49	151.78	93.15	72.84	57.24
	Stress [MPa]	3 266.56	1 190.40	730.55	571.31	448.97
	Extension [mm]	21.03	10.97	7.84	6.26	5.22
	Strain [%]	4.21	2.19	1.57	1.25	1.04
PA	Force [N]	198.07	-	196.65	-	196.38
	Stress [MPa]	806.12	-	800.35	-	799.26
	Extension [mm]	87.67	-	84.36	-	85.12
	Strain [%]	17.53	-	16.87	-	17.02
PET	Force [N]	261.15	248.13	251.72	249.94	242.55
	Stress [MPa]	1 061.22	1 008.32	1 022.88	1 015.67	985.63
	Extension [mm]	67.90	65.51	66.63	67.05	66.68
	Strain [%]	13.58	13.10	13.33	13.41	13.34

Table 5. Mechanical results of rupture under ultraviolet incidence for all fibres.

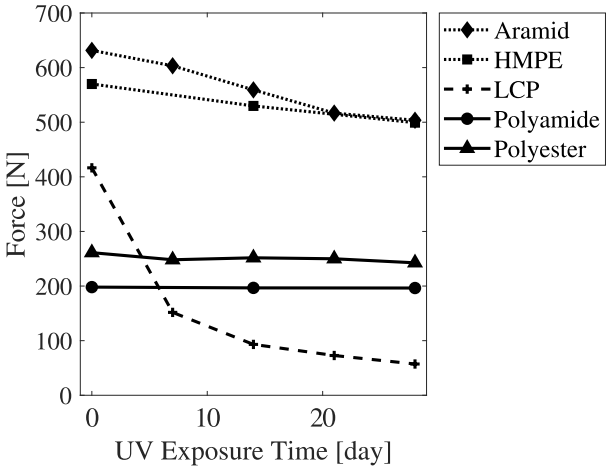

Figure 4. Break strength degradation due to ultraviolet exposure for all fibres.

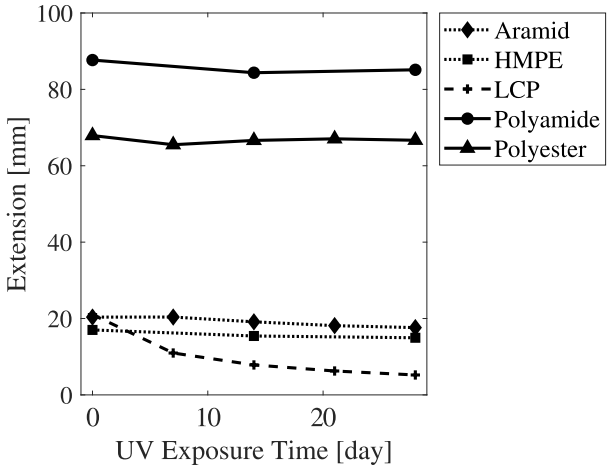

Figure 5. Break extension degradation due to ultraviolet exposure for all fibres.

the best stability against UV incidence. They show a decrease in mechanical behaviour but in a very restrained, almost minimal manner.

On the contrary, for Aramid and HMPE samples, there was a more significant decrease in mechanical strength as compared to polyamide and polyester. For these materials, Aramid and HMPE, rupture elongation remain relatively constant even with the increased duration of UV exposure. Concerning rupture strength, the 28-day condition (maximum UV exposure in the study) represents a reduction of approximately 20 % from the virgin rupture value for Aramid and 13 % for HMPE.

The LCP is the material whose mechanical performance degrades the most under UV exposure. The same decrease in rupture force is reflected in rupture elongation with the increased duration of UV exposure for LCP fibres. After 28 days of UV exposure, the residual rupture value is 86 % lower than the initial condition (without UV exposure).

Fibres exhibit varying orders of magnitude in terms of both rupture strength and rupture elongation. Normalising the results allows a comparison between different fibres. The normalisation process involves dividing all results obtained for different UV exposure durations of a particular fibre by its virgin rupture

Material	Normalised Property	0 days	7 days	14 days	21 days	28 days
Aramid	Force [N N^{-1}]	1.000	0.955	0.885	0.818	0.797
	Extension [mm mm^{-1}]	1.000	1.001	0.940	0.891	0.865
HMPE	Force [N N^{-1}]	1.000	-	0.930	-	0.876
	Extension [mm mm^{-1}]	1.000	-	0.907	-	0.880
LCP	Force [N N^{-1}]	1.000	0.364	0.224	0.175	0.137
	Extension [mm mm^{-1}]	1.000	0.522	0.373	0.298	0.248
Polyamide	Force [N N^{-1}]	1.000	-	0.993	-	0.991
	Extension [mm mm^{-1}]	1.000	-	0.962	-	0.971
Polyester	Force [N N^{-1}]	1.000	0.950	0.964	0.957	0.929
	Extension [mm mm^{-1}]	1.000	0.965	0.981	0.987	0.982

TABLE 6. Dimensionless mechanical rupture results under ultraviolet incidence for all fibres.

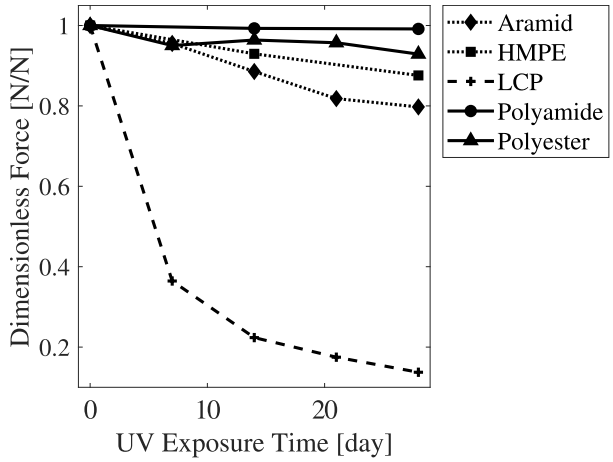

FIGURE 6. Dimensionless break strength degradation due to ultraviolet exposure for all fibres.

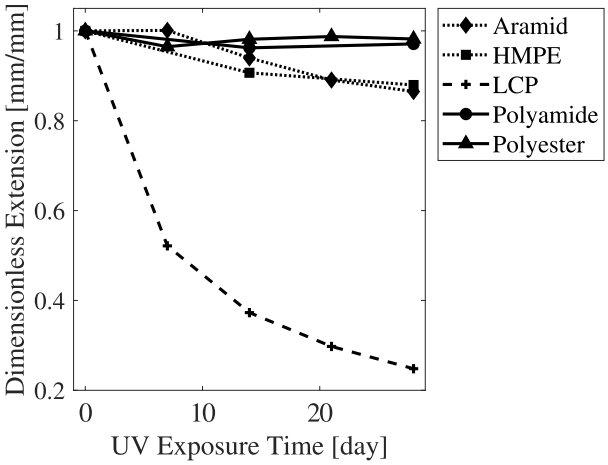

FIGURE 7. Dimensionless break extension degradation due to ultraviolet exposure for all fibres.

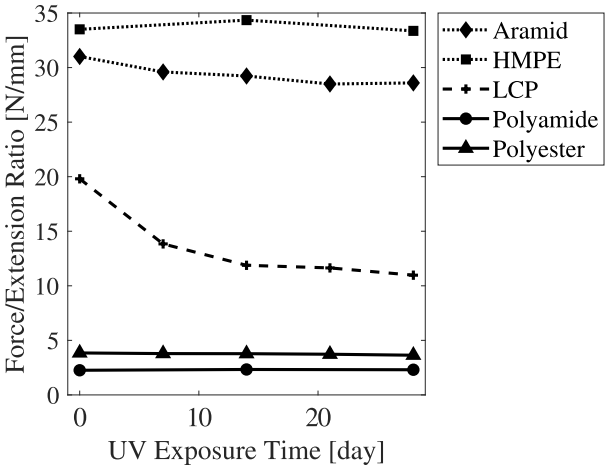

FIGURE 8. Force/extension ratio at break due to ultraviolet exposure for all fibres.

value (i.e. the rupture value without ultraviolet exposure). Consequently, all curves originate from a unitary value, and represent the evolution of behaviour with UV exposure in proportion to the reference condition (0 days).

The normalised data are presented in Table 6, and plotted in Figure 6 for break strenght and Figure 7 for break extension. It can be observed that polyester and polyamide, both in terms of strength and extension criteria, are the most stable fibres under ultraviolet radiation. HMPE and Aramid show a slightly higher degradation, but still in a mild manner. In the case of LCP, the mechanical behaviour changes abruptly; the fibre undergoes significant degradation due to the ultraviolet exposure in terms of rupture force and elongation.

The values presented in Table 6, along with the general graphical behaviour in Figures 6 and 7, allow for a potential interpretation that UV exposure decreases the rupture force for each fibre, similarly to the reduction in rupture elongation. Thus, it is possible that when plotting the ratio of force to extension, this value remains approximately constant even with an increase in the UV exposure time. It is noteworthy that this force-to-extension ratio gives a unit of N mm^{-1}, but it does not represent a direct or equivalent stiffness of the fibre, as these materials are viscoelastic and do not exhibit linearity in the stress-strain curve. Hence, Figure 8 is proposed, illustrating the ratio of rupture-

Model	Parameter	Aramid	HMPE	LCP	Polyamide	Polyester
Linear	A	-4.89	-2.53	-11.39	-0.06	-0.51
	B	631.36	568.39	317.78	197.87	257.78
	R^2	0.9768	0.9940	0.7188	0.8658	0.6814
Power	A	-1.13×10^{-2}	-7.20×10^{-3}	-1.13×10^{-1}	-5.46×10^{-4}	-3.70×10^{-3}
	B	560.05	525.16	118.19	196.83	250.53
	R^2	0.5487	0.8310	0.8510	0.9884	0.7586
Exponential	A	-8.70×10^{-3}	-4.70×10^{-3}	-6.72×10^{-2}	-3.06×10^{-4}	-2.00×10^{-3}
	B	633.21	568.70	306.57	197.87	257.77
	R^2	0.9786	0.9966	0.8974	0.8662	0.6830
Reciprocal	A	1.55×10^{-5}	8.89×10^{-6}	5.33×10^{-4}	1.55×10^{-6}	7.97×10^{-6}
	B	1.60×10^{-3}	1.80×10^{-3}	2.70×10^{-3}	5.10×10^{-3}	3.90×10^{-3}
	R^2	0.9791	0.9984	0.9965	0.8666	0.6843
Michaelis-Menten	A	542.97	514.05	82.44	196.51	248.04
	B	-1.40×10^{-6}	-9.81×10^{-7}	-8.02×10^{-6}	-7.84×10^{-8}	-5.02×10^{-7}
	R^2	0.4459	0.7835	0.5431	0.9778	0.7202

Table 7. Results for the mathematical models for all fibres.

force to rupture-elongation [N mm^{-1}] for each of the fibres over the course of the UV exposure time.

As observed in Figure 8, with the exception of LCP, all other fibres indeed maintain an approximately constant force/extension ratio even with increasing UV exposure time. This implies that the degradation of mechanical rupture behaviour due to ultraviolet exposure is linear in relation to the constitutive behaviour of the material. In other words, for the studied durations, it is evident that longer exposure to ultraviolet light leads to greater mechanical degradation. However, Figure 8 demonstrates that, for most fibres, this degradation occurs simultaneously and similarly for both the force and extension. In this context, considering a characteristic stiffness of the material (concept of derivative along the stress-strain curve), it is as if the degradation restricts the continuation of the test on the curve, anticipating the moment of rupture compared to the condition without UV exposure.

The experimental results presented can be mathematically modelled as described in Section 2.4, both for the force and extension data. In this case, the mathematical modelling study is conducted only for the force data. Applying the methodology described earlier, the results are obtained and shown in Table 7 in terms of coefficients for each model and their respective coefficients of determination (R^2). It is noteworthy that for all expressions/models, y refers to the force value in Newton, and x refers to the exposure time in day.

The results pertaining to the coefficients of each model have been obtained. It is noteworthy that in Table 7, the best model for each fibre (having the highest coefficient of determination, R^2) is highlighted: in red for aramid, in green for HMPE, in blue for LCP, in magenta for polyamide, and in cyan for polyester. For Aramid, HMPE, and LCP fibres, the reciprocal model was the one that best fit the data within the range

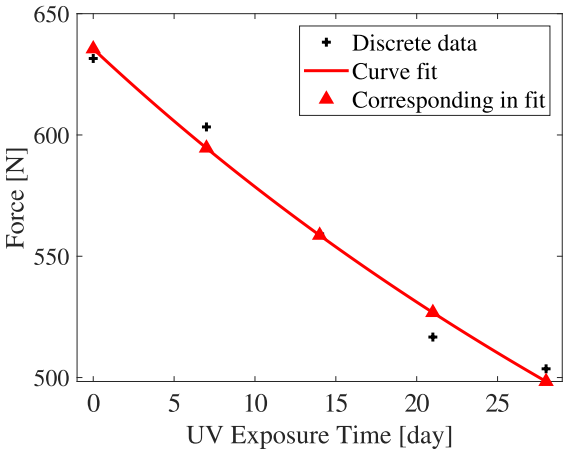

Figure 9. Reciprocal mathematical model for Aramid, force *versus* UV exposure time.

addressed in this study. Meanwhile, for polyamide and polyester fibres, the best fit is achieved with the power model for the studied interval.

For each fibre, the best-fitted equation can be highlighted, along with the curve fitting of this model compared to the experimental data. Equation (3) and Figure 9 mathematically models the force *versus* UV exposure time for Aramid:

$$y = \frac{1}{1.60 \times 10^{-3} + 1.55 \times 10^{-5} \cdot x}. \tag{3}$$

Similarly, for HMPE fibres, Equation (4) and Figure 10 are obtained, also in a reciprocal model:

$$y = \frac{1}{1.80 \times 10^{-3} + 8.89 \times 10^{-6} \cdot x}. \tag{4}$$

For LCP fibres, the reciprocal model is still used for modelling, and Equation (5) and Figure 11 are presented:

$$y = \frac{1}{2.70 \times 10^{-3} + 5.33 \times 10^{-4} \cdot x}. \tag{5}$$

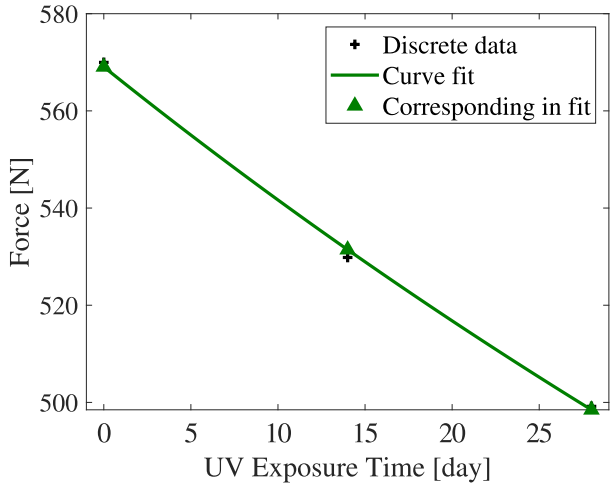

FIGURE 10. Reciprocal mathematical model for HMPE, force *versus* UV exposure time.

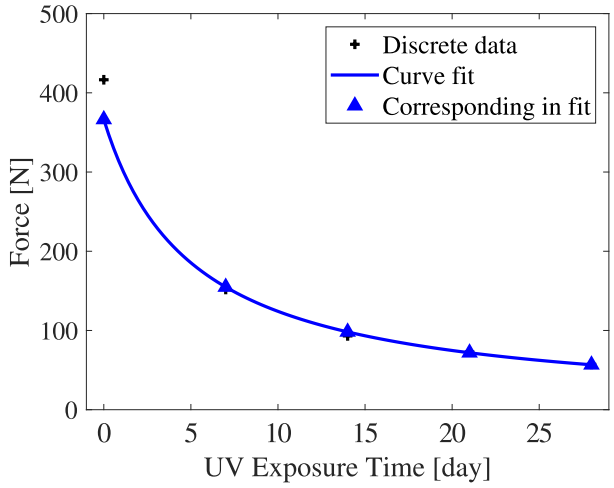

FIGURE 11. Reciprocal mathematical model for LCP, force *versus* UV exposure time.

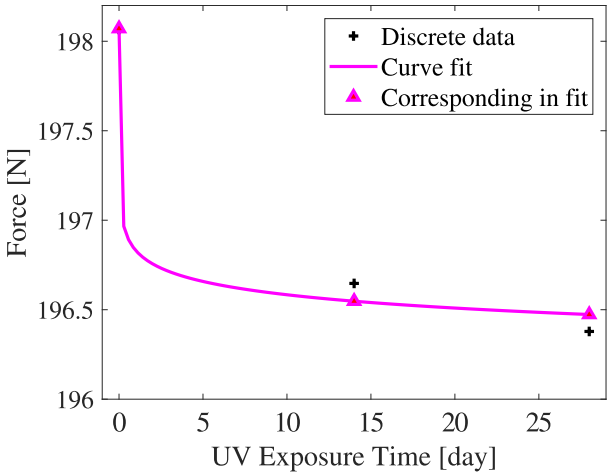

FIGURE 12. Power mathematical model for polyamide, force *versus* UV exposure time.

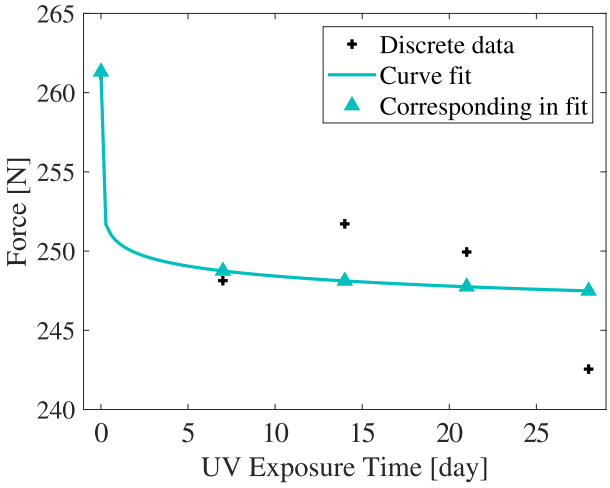

FIGURE 13. Power mathematical model for polyester, force *versus* UV exposure time.

What is observed in the parameterisations made for Aramid, HMPE, and LCP with reciprocal models is that the curve fits very well to the data and exhibits certain homogeneity, where the decrease in rupture force is a gradual influence of the ultraviolet exposure throughout the entire study period.

Now, for the polyamide fibre, the best model was the power model, Equation (6) and Figure 12 depicts these results:

$$y = 196.83 \cdot x^{-5.46\times10^{-4}}. \tag{6}$$

Similarly, the results for polyester are addressed (also a power model), in Equation (7) and Figure 13:

$$y = 250.53 \cdot x^{-3.70\times10^{-3}}. \tag{7}$$

In general, the behaviour of curves in the power model is naturally different from the behaviour of curves in the reciprocal model. Note that the homogeneity of the decrease in value is not present for polyamide (Figure 12) and polyester (Figure 13), unlike the models for Aramid, HMPE, and LCP fibres.

It is worth noting that in the previously presented experimental data, polyamide and polyester fibres already showed better stability under UV incidence. What the mathematical model allows us to infer is that these fibres degrade substantially upon initial exposure to UV, after which the force values tend to remain stable even with increasing exposure time, or show only a minimal decrease in the force values.

However, it is important to highlight a caveat regarding polyester. The mathematical model for polyester fibres is significantly limited across all types of curves. In Table 7, it can be observed that the coefficients of determination (R^2) are substantially lower for all polyester models when compared to other fibres. Therefore, for this fibre, the model may not be the most suitable for predicting polyester failure under UV exposure. Nevertheless, in comparative terms, the best R^2 provides an approximate representation of the behaviour (Figure 13).

For a visual representation, all the obtained models for predicting degradation in terms of breaking force *versus* UV exposure time are shown in Figure 14, in

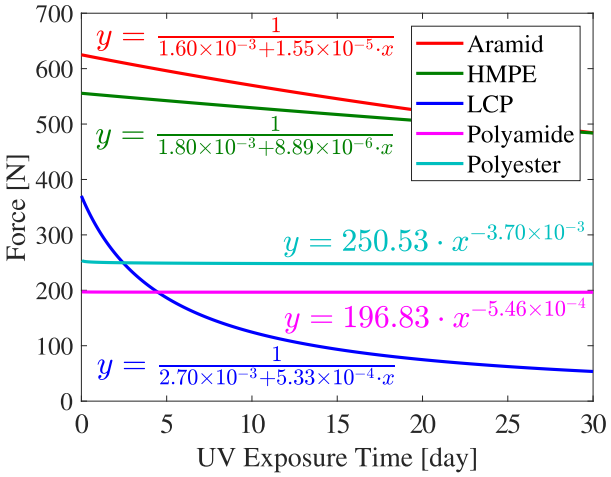

Figure 14. Mathematical models for all fibres, force *versus* UV exposure time.

the same graph scale for all fibres. This plot allows for a general visualisation of the behaviours, for example, helping to perceive that the instantaneous degradation of polyamide and polyester on first UV exposure in relation to the condition without UV (shown in Figures 12 and 13, respectively) occurs on a small force scale, which when compared in the general view of all fibres becomes negligible, indicating strong stability to UV exposure of these fibres.

4. Conclusion

In conclusion, the mechanical characterisation of aramid, HMPE, LCP, polyamide, and polyester fibres under different durations of ultraviolet (UV) exposure provides insights into their behaviour and degradation mechanisms. The initial mechanical results offer a baseline for comparison, demonstrating the properties of each fibre mentioned in the material descriptions.

Regarding the impact of UV exposure on these fibres over different time intervals, it is notable that LCP fibres exhibit a substantial decrease in mechanical properties as UV exposure duration increases, without showing any stabilisation for the times tested. For the most extended period of UV exposure (28 days), there is an 86 % reduction in the reference value (0 days of UV exposure).

Polyamide and polyester stand out for their stability against UV incidence, showing minimal degradation in both the rupture force and elongation. Aramid and HMPE, while exhibiting a more significant decrease in rupture force, maintain relatively constant rupture elongation even with prolonged UV exposure. The normalisation of results allows a direct comparison between the different fibres, including viewing the reduction percentiles compared to the reference condition.

The concept of force/extension ratio illustrates that, except for LCP, this ratio remains approximately constant for all fibres with increasing UV exposure time. This implies a linear degradation in mechanical rupture behaviour concerning the constitutive behaviour of the materials, as if UV degradation restricted the material's stress-strain curve without changing its shape. This is verified for Aramid, HMPE, polyamide, and polyester when making linear coefficients for the data of the force/extension ratio. For these materials, values of -0.085, -0.005, 0.002, and -0.007 were found, respectively, and these values are close to zero, indicating a constant trend without a significant angular coefficient. For LCP, there is a considerable value of -0.283.

The curve fitting of force data further elucidates the degradation patterns. The reciprocal model fits well for Aramid, HMPE, and LCP, indicating a gradual effect of UV exposure on rupture force. In contrast, the power model is more suitable for polyamide and polyester, suggesting an initial substantial degradation followed by stable or minimally decreasing force values, coinciding with the fibres most resistant to UV incidence.

In summary, the experimental and modelling results collectively contribute to a comprehensive understanding of how different fibres respond to UV exposure. For future studies, these effects should be investigated for larger structural elements, such as legs and subropes used to manufacture offshore mooring ropes. Because ultraviolet exposure can be understood as a surface phenomenon, which, for larger structural elements, increases both the incidence area and the resistant section simultaneously.

Acknowledgements

This study was financed in part by the Coordenação de Aperfeiçoamento de Pessoal de Nível Superior – Brasil (CAPES) – Finance Code 001. Thanks also to the funding agencies: CNPq, Finep, and FAPERGS.

References

[1] C. J. M. Del Vecchio. *Light weight materials for deep water moorings*. Ph.D. thesis, University of Reading, UK, 1992.

[2] M. M. Winkler, H. A. McKenna. The polyester rope taut leg mooring concept: A feasible means for reducing deepwater mooring cost and improving stationkeeping performance. In *Offshore Technology Conference*, pp. OTC–7708–MS. Texas, USA, 1995. https://doi.org/10.4043/7708-MS

[3] H. A. McKenna, J. W. S. Hearle, N. O'Hear. *Handbook of fibre rope technology*, vol. 34. Woodhead Publishing, UK, 2004.

[4] E. L. V. Louzada, C. E. M. Guilherme, F. T. Stumpf. Evaluation of the fatigue response of polyester yarns after the application of abrupt tension loads. *Acta Polytechnica CTU Proceedings* **7**:76–78, 2016. https://doi.org/10.14311/APP.2017.7.0076

[5] C. Wibner, T. Versavel, I. Masetti. Specifying and testing polyester mooring rope for the barracuda and caratinga FPSO deepwater mooring systems. In *Offshore Technology Conference*, pp. OTC–15139–MS. Texas, USA, 2003. https://doi.org/10.4043/15139-MS

[6] S. J. Banfield, N. F. Casey, R. Nataraja. Durability of polyester deepwater mooring rope. In *Offshore Technology Conference*, pp. OTC–17510–MS. Texas, USA, 2005. https://doi.org/10.4043/17510-MS

[7] T. M. Schmidt, C. Bianchini, M. M. C. Forte, et al. Socketing of polyester fibre ropes with epoxy resins for deep-water mooring applications. *Polymer Testing* **25**(8):1044–1051, 2006. https://doi.org/10.1016/j.polymertesting.2006.07.003

[8] P. Davies, P. Baron, K. Salomon, et al. Influence of fibre stiffness on deepwater mooring line response. In *27th International Conference on Offshore Mechanics and Arctic Engineering*, pp. 179–187. Portugal, 2008. https://doi.org/10.1115/OMAE2008-57147

[9] A. Tahar, D. Sidarta, A. Ran. Dual stiffness approach for polyester mooring line analysis in time domain. In *31st International Conference on Ocean, Offshore and Arctic Engineering*, pp. 513–521. Brazil, 2012. https://doi.org/10.1115/OMAE2012-83662

[10] C. T. Kwan, P. Devlin, P.-L. Tan, K. Huang. Stiffness modeling, testing, and global analysis for polyester mooring. In *31st International Conference on Ocean, Offshore and Arctic Engineering*, pp. 777–785. Brazil, 2012. https://doi.org/10.1115/OMAE2012-84159

[11] M. B. Bastos. Improved high tenacity/high modulus polyester for stiffer mooring ropes. In *2013 MTS/IEEE OCEANS – Bergen*, pp. 1–5. Bergen, Norway, 2013. https://doi.org/10.1109/OCEANS-Bergen.2013.6607949

[12] S. Xu, S. Wang, H. Liu, et al. Experimental evaluation of the dynamic stiffness of synthetic fibre mooring ropes. *Applied Ocean Research* **112**:102709, 2021. https://doi.org/10.1016/j.apor.2021.102709

[13] S. R. Ghoreishi, P. Cartraud, P. Davies, T. Messager. Analytical modeling of synthetic fiber ropes subjected to axial loads. Part I: A new continuum model for multilayered fibrous structures. *International Journal of Solids and Structures* **44**(9):2924–2942, 2007. https://doi.org/10.1016/j.ijsolstr.2006.08.033

[14] S. R. Ghoreishi, P. Davies, P. Cartraud, T. Messager. Analytical modeling of synthetic fiber ropes. Part II: A linear elastic model for 1 + 6 fibrous structures. *International Journal of Solids and Structures* **44**(9):2943–2960, 2007. https://doi.org/10.1016/j.ijsolstr.2006.08.032

[15] A. Tahar, M. H. Kim. Coupled-dynamic analysis of floating structures with polyester mooring lines. *Ocean Engineering* **35**(17–18):1676–1685, 2008. https://doi.org/10.1016/j.oceaneng.2008.09.004

[16] J. Davidson, J. V. Ringwood. Mathematical modelling of mooring systems for wave energy converters – A review. *Energies* **10**(5):666, 2017. https://doi.org/10.3390/en10050666

[17] S. D. Weller, S. J. Banfield, J. Canedo. Parameter estimation for synthetic rope models. In *37th International Conference on Ocean, Offshore and Arctic Engineering*, pp. OMAE2018–78606. Spain, 2018. https://doi.org/10.1115/OMAE2018-78606

[18] J. F. Beltran, E. B. Williamson. Numerical simulation of damage localization in polyester mooring ropes. *Journal of Engineering Mechanics* **136**(8):945–959, 2010. https://doi.org/10.1061/(ASCE)EM.1943-7889.0000129

[19] J. F. Beltran, E. B. Williamson. Numerical procedure for the analysis of damaged polyester ropes. *Engineering Structures* **33**(5):1698–1709, 2011. https://doi.org/10.1016/j.engstruct.2011.02.007

[20] W. Huang, H. Liu, Y. Lian, L. Li. Modeling nonlinear creep and recovery behaviors of synthetic fiber ropes for deepwater moorings. *Applied Ocean Research* **39**:113–120, 2013. https://doi.org/10.1016/j.apor.2012.10.004

[21] L. Xiong, X. Li, J. Yang, W. Lu. Numerical simulation of nonlinearity and viscoelasticity of synthetic fibre rope for taut moorings in deep water. *Ships and Offshore Structures* **13**(2):132–142, 2017. https://doi.org/10.1080/17445302.2017.1328757

[22] I. Ćatipović, N. Alujević, S. Rudan, V. Slapničar. Numerical modelling for synthetic fibre mooring lines taking elongation and contraction into account. *Journal of Marine Science and Engineering* **9**(4):417, 2021. https://doi.org/10.3390/jmse9040417

[23] D. M. da Cruz, C. E. M. Guilherme, F. T. Stumpf, M. B. Bastos. Numerical assessment of mechanical behavior of mooring lines using hybrid synthetic fiber-rope segments. In *Offshore Technology Conference*, pp. OTC–31906–MS. Texas, USA, 2022. https://doi.org/10.4043/31906-MS

[24] F. T. Stumpf, C. E. M. Guilherme, D. M. da Cruz, et al. A general constitutive model for the numerical simulation of different synthetic fibres used in offshore mooring. *Ships and Offshore Structures* **18**(9):1338–1344, 2023. https://doi.org/10.1080/17445302.2022.2116766

[25] H. H. Pham. Numerical modeling of a mooring line system for an offshore floating wind turbine in Vietnamese sea conditions using nonlinear materials. *Water Science and Engineering* **17**(3):300–308, 2024. https://doi.org/10.1016/j.wse.2023.10.004

[26] D. M. da Cruz, T. L. Popiolek Júnior, M. A. Barreto, et al. Evaluation of energy models for numerical simulation of the mechanical behavior of polyester multifilaments. *The Journal of Engineering and Exact Sciences* **9**(1):15321–01e, 2023. https://doi.org/10.18540/jcecvl9iss1pp15321-01e

[27] H. Liu, W. Huang, Y. Lian, L. Li. An experimental investigation on nonlinear behaviors of synthetic fiber ropes for deepwater moorings under cyclic loading. *Applied Ocean Research* **45**:22–32, 2014. https://doi.org/10.1016/j.apor.2013.12.003

[28] C. Ji, Z. Yuan. Experimental study of a hybrid mooring system. *Journal of Marine Science and Technology* **20**:213–225, 2015. https://doi.org/10.1007/s00773-014-0260-7

[29] J. Koto, C. L. Siow. Experimental study of polyester mooring lines. *Journal of Ocean, Mechanical and Aerospace-science and engineering (JOMAse)* **50**(1):8–13, 2017. https://doi.org/10.36842/jomase.v50i1.162

[30] J. P. Duarte, C. E. M. Guilherme, A. H. M. F. T. da Silva, et al. Lifetime prediction of aramid yarns applied to offshore mooring due to purely hydrolytic degradation. *Polymers and Polymer Composites* **27**(8):518–524, 2019. https://doi.org/10.1177/0967391119851386

[31] S. Xu, K. Rezanejad, J. F. M. Gadelho, et al. Experimental investigation on a dual chamber floating oscillating water column moored by flexible mooring systems. *Ocean Engineering* **216**:108083, 2020. https://doi.org/10.1016/j.oceaneng.2020.108083

[32] E. d. S. Belloni, F. M. Clain, C. E. M. Guilherme. Post-impact mechanical characterization of HMPE yarns. *Acta Polytechnica* **61**(3):406–414, 2021. https://doi.org/10.14311/AP.2021.61.0406

[33] D. M. da Cruz, F. M. Clain, C. E. M. Guilherme. Experimental study of the torsional effect for yarn break load test of polymeric multifilaments. *Acta Polytechnica* **62**(5):538–548, 2022. https://doi.org/10.14311/AP.2022.62.0538

[34] H. Zhang, J. Zeng, S. Tong, et al. Dynamic stiffness of polyester fiber mooring ropes: Experimental investigation based on radial basis function neural networks. *Ocean Engineering* **280**:114833, 2023. https://doi.org/10.1016/j.oceaneng.2023.114833

[35] D. M. da Cruz, A. Penaquioni, L. B. Zangalli, et al. Non-destructive testing of high-tenacity polyester sub-ropes for mooring systems. *Applied Ocean Research* **134**:103513, 2023. https://doi.org/10.1016/j.apor.2023.103513

[36] I. Melito, D. M. da Cruz, E. d. S. Belloni, et al. The effects of mechanical degradation on the quasi static and dynamic stiffness of polyester yarns. *Engineering Solid Mechanics* **11**(3):243–252, 2023. https://doi.org/10.5267/j.esm.2023.4.001

[37] D. M. da Cruz, M. A. Barreto, L. B. Zangalli, et al. Experimental study of creep behavior at high temperature in different HMPE fibers used for offshore mooring. In *Offshore Technology Conference Brasil*, pp. OTC–32760–MS. Brazil, 2023. https://doi.org/10.4043/32760-MS

[38] B. G. Achhammer, F. W. Reinhart, G. M. Kline. Mechanism of the degradation of polyamides. *Journal of Applied Chemistry* **1**(7):301–320, 1951. https://doi.org/10.1002/jctb.5010010704

[39] S. Ray, R. P. Cooney. Chapter 9 – Thermal degradation of polymer and polymer composites. In *Handbook of Environmental Degradation of Materials (Third Edition)*, pp. 185–206. William Andrew Publishing, 2018. https://doi.org/10.1016/B978-0-323-52472-8.00009-5

[40] A. L. Andrady, P. W. Barnes, J. F. Bornman, et al. Oxidation and fragmentation of plastics in a changing environment; from UV-radiation to biological degradation. *Science of The Total Environment* **851**(Part 2):158022, 2022. https://doi.org/10.1016/j.scitotenv.2022.158022

[41] G. Hahn, A. H. M. d. F. T. da Silva, F. T. Stumpf, C. E. M. Guilherme. Evaluation of residual strength of polymeric yarns subjected to previous impact loads. *Acta Polytechnica* **62**(4):473–478, 2022. https://doi.org/10.14311/AP.2022.62.0473

[42] Y. Duan, J. Li, W. Zhong, et al. Effects of compaction and UV exposure on performance of acrylate/glass-fiber composites cured layer by layer. *Journal of Applied Polymer Science* **123**(6):3799–3805, 2012. https://doi.org/10.1002/app.34909

[43] T. Lu, E. Solis-Ramos, Y. Yi, M. Kumosa. UV degradation model for polymers and polymer matrix composites. *Polymer Degradation and Stability* **154**:203–210, 2018. https://doi.org/10.1016/j.polymdegradstab.2018.06.004

[44] Y. C. Ching, T. M. S. Udenni Gunathilake, K. Y. Ching, et al. 18 – Effects of high temperature and ultraviolet radiation on polymer composites. In *Durability and Life Prediction in Biocomposites, Fibre-Reinforced Composites and Hybrid Composites*, pp. 407–426. Woodhead Publishing, 2019. https://doi.org/10.1016/B978-0-08-102290-0.00018-0

[45] F. Hulderman, J. S. Sanghera, J. D. Mackenzie. The effect of UV radiation on the mechanical strength of As_2Se_3 glass fibers. *Journal of Non-Crystalline Solids* **127**(3):312–322, 1991. https://doi.org/10.1016/0022-3093(91)90484-N

[46] M. M. Shokrieh, A. Bayat. Effects of ultraviolet radiation on mechanical properties of glass/polyester composites. *Journal of Composite Materials* **41**(20):2443–2455, 2007. https://doi.org/10.1177/0021998307075441

[47] S. Lohani, N. Shubham, R. K. Prusty, B. C. Ray. Effect of ultraviolet radiations on interlaminar shear strength and thermal properties of glass fiber/epoxy composites. *Materials Today: Proceedings* **43**(Part 1):524–529, 2021. https://doi.org/10.1016/j.matpr.2020.12.028

[48] T. Agnhage, Y. Zhou, J. Guan, et al. Bioactive and multifunctional textile using plant-based madder dye: Characterization of UV protection ability and antibacterial activity. *Fibers and Polymers* **18**:2170–2175, 2017. https://doi.org/10.1007/s12221-017-7115-x

[49] S. Eyupoglu. *Sustainability in the textile and apparel industries: Sourcing natural raw materials*, chap. Sustainable plant-based natural fibers, pp. 27–48. Springer International Publishing, 2020. https://doi.org/10.1007/978-3-030-38541-5_2

[50] E. Karaca, A. S. Hockenberger. Analysis of the fracture morphology of polyamide, polyester, polypropylene, and silk sutures before and after implantation in vivo. *Journal of Biomedical Materials Research Part B: Applied Biomaterials* **87B**(2):580–589, 2008. https://doi.org/10.1002/jbm.b.31136

[51] K. A. El-Farahaty, E. A. Seisa, S. G. El-Sheikh. Influence of wavelength and temperature on the optical and some structural properties of polyester and polyamide surgical suture fibers. *Optical Materials* **32**(9):928–935, 2010. https://doi.org/10.1016/j.optmat.2010.01.027

[52] S. Afewerki, S. V. Harb, T. D. Stocco, et al. Chapter 5 – Polymers for surgical sutures. In *Advanced Technologies and Polymer Materials for Surgical Sutures*, Woodhead Publishing Series in Biomaterials, pp. 95–128. Woodhead Publishing, 2023. https://doi.org/10.1016/B978-0-12-819750-9.00004-8

[53] M. M. Jafari, S. Jahandari, T. Ozbakkaloglu, et al. Mechanical properties of polyamide fiber-reinforced lime – cement concrete. *Sustainability* **15**(15):11484, 2023. https://doi.org/10.3390/su151511484

[54] H. Jia, Y. Sheng, P. Guo, et al. Effect of synthetic fibers on the mechanical performance of asphalt mixture: A review. *Journal of Traffic and Transportation Engineering (English Edition)* **10**(3):331–348, 2023. https://doi.org/10.1016/j.jtte.2023.02.002

[55] D. A. Martin, M. Obstalecki, P. Kurath, G. P. Horn. An approach for quantifying dynamic properties and simulated deployment loading of fire service escape rope systems. *Experimental Techniques* **40**:367–379, 2016. https://doi.org/10.1007/s40799-016-0041-9

[56] A. Novikova, F. Joseph, D. Cleveland. Rock-climbing apparel: An analysis of current clothing options and future strategies for the design of rock-climbing clothing. *International Journal of Fashion Design, Technology and Education* **17**(2):193–201, 2024. https://doi.org/10.1080/17543266.2023.2261023

[57] H. Tanizaki, K. Takagi, C. Oiwa, et al. Experimental investigation of temperature-dependent hysteresis of fishing-line artificial muscle (twisted and coiled polymer fiber) actuator. In *Electroactive Polymer Actuators and Devices (EAPAD) XXI*, vol. 10966, pp. 68–74. 2019. https://doi.org/10.1117/12.2513834

[58] Y. An, T. Kajiwara, A. Padermshoke, et al. Environmental degradation of nylon, poly(ethylene terephthalate) (PET), and poly(vinylidene fluoride) (PVDF) fishing line fibers. *ACS Applied Polymer Materials* **5**(6):4427–4436, 2023. https://doi.org/10.1021/acsapm.3c00552

[59] S. D. Weller, L. Johanning, P. Davies, S. J. Banfield. Synthetic mooring ropes for marine renewable energy applications. *Renewable Energy* **83**:1268–1278, 2015. https://doi.org/10.1016/j.renene.2015.03.058

[60] M. B. Bastos, E. B. Fernandes, A. L. N. da Silva. Performance fibers for deep water offshore mooring ropes: Evaluation and analysis. In *OCEANS 2016 – Shanghai*. China, 2016. https://doi.org/10.1109/OCEANSAP.2016.7485612

[61] V. S. Matveev, G. A. Budnitskii, G. P. Mashinskaya, et al. Structural and mechanical characteristics of aramid fibres for bullet-proof vests. *Fibre Chemistry* **29**(6):381–384, 1997. https://doi.org/10.1007/BF02418874

[62] S. Vignesh, R. Surendran, T. Sekar, B. Rajeswari. Ballistic impact analysis of graphene nanosheets reinforced kevlar-29. *Materials Today: Proceedings* **45**(Part 2):788–793, 2021. https://doi.org/10.1016/j.matpr.2020.02.808

[63] P. G. Riewald. Performance analysis of an aramid mooring line. In *Offshore Technology Conference*, pp. OTC–5187–MS. Texas, USA, 1986. https://doi.org/10.4043/5187-MS

[64] C. T. Berryman, R. M. Dupin, N. S. Gerrits. Laboratory study of used HMPE MODU mooring lines. In *Offshore Technology Conference*, pp. OTC–14245–MS. Texas, USA, 2002. https://doi.org/10.4043/14245-MS

[65] S. Leite, J. Boesten. HMPE mooring lines for deepwater MODUs. In *Offshore Technology Conference Brasil*, pp. OTC–22486–MS. Brazil, 2011. https://doi.org/10.4043/22486-MS

[66] M. Vlasblom, J. Boesten, S. Leite, P. Davies. Development of HMPE fiber for permanent deepwater offshore mooring. In *Offshore Technology Conference*, pp. OTC–23333–MS. Texas, USA, 2012. https://doi.org/10.4043/23333-MS

[67] H. van der Werff, U. Heisserer. 3 – High-performance ballistic fibers: Ultra-high molecular weight polyethylene (UHMWPE). In *Advanced Fibrous Composite Materials for Ballistic Protection*, pp. 71–107. Woodhead Publishing, 2016. https://doi.org/10.1016/B978-1-78242-461-1.00003-0

[68] Y. Lian, B. Zhang, J. Ji, et al. Experimental investigation on service safety and reliability of full-scale HMPE fiber slings for offshore lifting operations. *Ocean Engineering* **285**(Part 2):115447, 2023. https://doi.org/10.1016/j.oceaneng.2023.115447

[69] F. Sloan. 5 – Liquid crystal aromatic polyester-arylate (LCP) fibers: Structure, properties, and applications. In *Structure and Properties of High-Performance Fibers*, Woodhead Publishing Series in Textiles, pp. 113–140. Woodhead Publishing, 2017. https://doi.org/10.1016/B978-0-08-100550-7.00005-X

[70] F. Sloan, S. Bull, R. Longerich. Design modifications to increase fatigue life of fiber ropes. In *Proceedings of OCEANS 2005 MTS/IEEE*, pp. 829–835. Washington, USA, 2005. https://doi.org/10.1109/OCEANS.2005.1639856

[71] S. Kery. Dynamic modeling of ship-to-ship and ship-to-pier mooring performance. *Marine Technology Society Journal* **52**(5):87–93, 2018. https://doi.org/10.4031/MTSJ.52.5.10

[72] A. Abbas, M. S. Anas, Z. Azam, et al. Analysis of material variation in the design of knitted sportswear compression stockings to escort thermo-physiological comfort using linear regression. *The Journal of The Textile Institute* **115**(1):56–65, 2022. https://doi.org/10.1080/00405000.2022.2157636

[73] A. A. Leal, R. Stämpfli, R. Hufenus. On the analysis of cut resistance in polymer-based climbing ropes: New testing methodology and resulting modes of failure. *Polymer Testing* **62**:254–262, 2017. https://doi.org/10.1016/j.polymertesting.2017.07.004

[74] D. M. da Cruz, A. H. M. F. T. da Silva, F. M. Clain, C. E. M. Guilherme. Experimental study on the behavior of polyamide multifilament subject to impact loads under different soaking conditions. *Engineering Solid Mechanics* **11**(1):23–34, 2022. https://doi.org/10.5267/j.esm.2022.11.001

[75] Y. Chevillotte, Y. Marco, G. Bles, et al. Fatigue of improved polyamide mooring ropes for floating wind turbines. *Ocean Engineering* **199**:107011, 2020. https://doi.org/10.1016/j.oceaneng.2020.107011

[76] S. A. Hosseini Ravandi, M. Valizadeh. 2 – Properties of fibers and fabrics that contribute to human comfort. In *Improving Comfort in Clothing*, pp. 61–78. Woodhead Publishing, 2011. https://doi.org/10.1533/9780857090645.1.61

[77] American Society for Testing and Materials. Standard practice for operating xenon arc lamp apparatus for exposure of materials. ASTM G155-21, 2021. https://doi.org/10.1520/G0155-21

[78] American Society for Testing and Materials. Standard practice for fluorescent ultraviolet (UV) lamp apparatus exposure of plastics. ASTM D4329-21, 2021. https://doi.org/10.1520/D4329-21

[79] International Organization for Standardization. Plastics – methods of exposure to laboratory light sources. ISO 4892-1:2024, 2024.

[80] American Society for Testing and Materials. Standard test method for breaking force and elongation of textile fabrics (strip method). ASTM D5035-11(2019), 2019. https://doi.org/10.1520/D5035-11R19

[81] Q-Lab Corporation. Technical bulletin LU-8160, 2016.

[82] American Society for Testing and Materials. Standard test methods for linear density of textile fibers. ASTM D1577-07(2018), 2018. https://doi.org/10.1520/D1577-07R18

[83] International Organization for Standardization. Textiles – standard atmospheres for conditioning and testing. ISO 139:2005, 2005.

[84] International Organization for Standardization. Textiles – yarns from packages – determination of single-end breaking force and elongation at break using constant rate of extension (CRE) tester. ISO 2062:2009, 2009.

[85] G. Ávila. *Introdução à análise matemática [In Portuguese; Introduction to mathematical analysis].* Editora Edgar Blucher, Brasil, 1999.

[86] R. M. L. R. F. Brasil, J. M. Balthazar, W. Góis. *Métodos numéricos e computacionais na prática de engenharias e ciências [In Portuguese; Numerical and computational methods in engineering and science practice].* Editora Edgar Blucher, Brasil, 2015.

[87] D. M. da Cruz, I. Melito, A. J. da Cruz Júnior, et al. Desenvolvimento de código aberto em Octave para ajustes de funções através de linearização e MMQ [In Portuguese; Open source development in Octave for function adjustments through linearization and OLS]. *E&S Engineering and Science* **13**(1):1–14, 2024. https://doi.org/10.18607/ES20241316896